

NACA TN 2950

# NATIONAL ADVISORY COMMITTEE FOR AERONAUTICS

TECHNICAL NOTE 2950

A NEW SHADOWGRAPH TECHNIQUE FOR  
THE OBSERVATION OF CONICAL FLOW PHENOMENA IN  
SUPERSONIC FLOW AND PRELIMINARY RESULTS

OBTAINED FOR A TRIANGULAR WING

By Eugene S. Love and Carl E. Grigsby

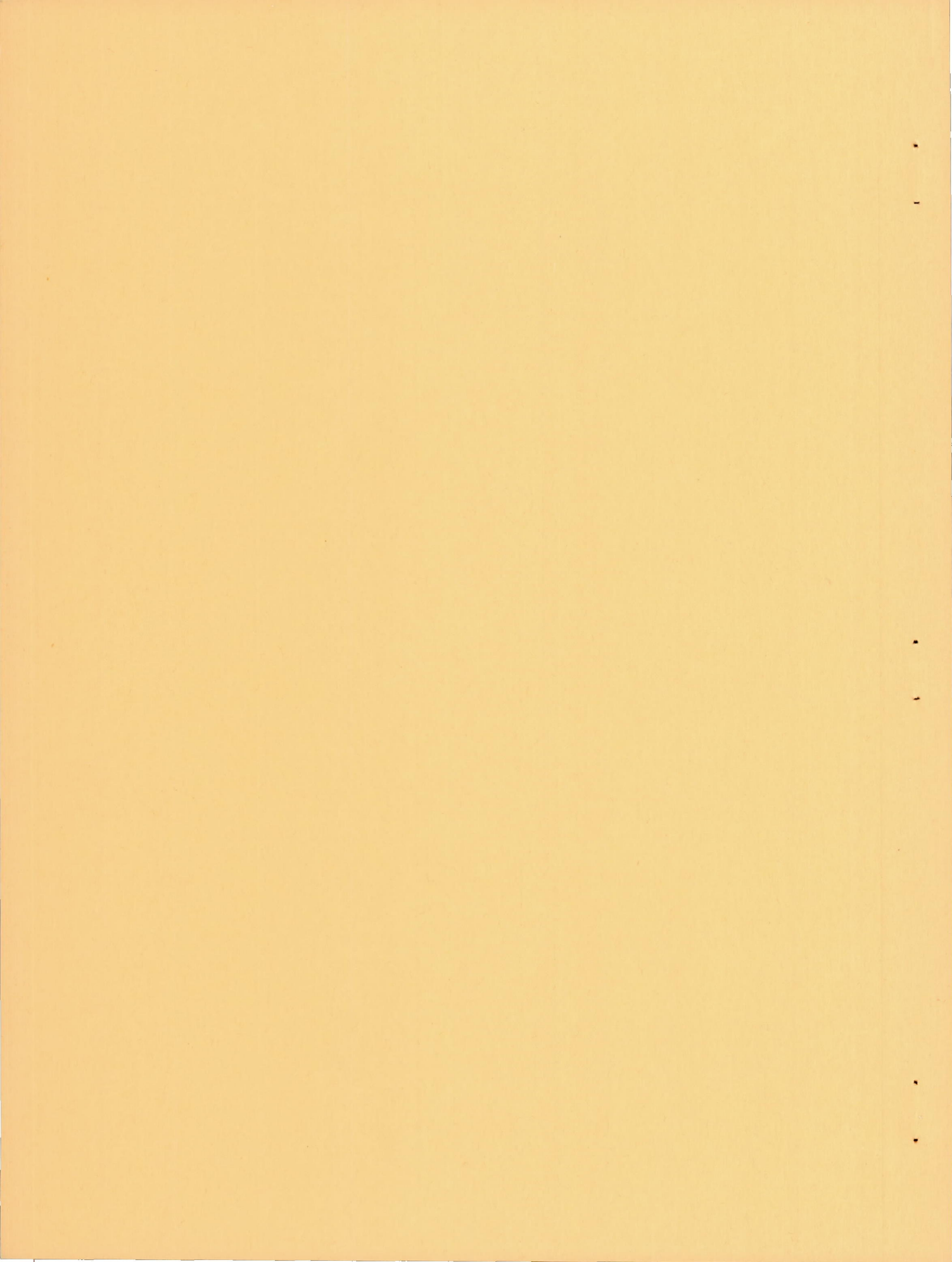
Langley Aeronautical Laboratory  
Langley Field, Va.



Washington

May 1953

**CASE FILE**  
**COPY**



## NATIONAL ADVISORY COMMITTEE FOR AERONAUTICS

TECHNICAL NOTE 2950

A NEW SHADOWGRAPH TECHNIQUE FOR  
THE OBSERVATION OF CONICAL FLOW PHENOMENA IN  
SUPERSONIC FLOW AND PRELIMINARY RESULTS  
OBTAINED FOR A TRIANGULAR WING

By Eugene S. Love and Carl E. Grigsby

## SUMMARY

A new shadowgraph technique for the observation of conical flow phenomena in supersonic flow is presented. The particular advantage of this technique over conventional types of shadowgraph or schlieren systems is that it permits observation of the conical flow phenomena in a plane normal or nearly normal to the axis of propagation. The principle of the shadowgraph is utilized by superimposing a conical light field upon a conical flow field in such a way as to project the shadowgraph on a propeller screen within the test section of the tunnel. Preliminary results are presented for a triangular wing of  $38^\circ$  half-apex angle.

## INTRODUCTION

In many wind-tunnel investigations at supersonic speeds the flow fields about the models are conical or nearly conical: for example, the flow fields created by cones, certain types and portions of other bodies of revolution, triangular wings, and sweptback wings. Within these flow fields certain flow phenomena often exist whose presence is indicated indirectly but which cannot be observed by ordinary optical methods (schlieren or shadowgraph) in a manner that permits a realistic picture of the phenomena, either in structure or location. One example of such phenomena is the shocks which have been observed to leave the trailing edge of triangular wings when viewed in plan form.

Schlieren photographs from tests made previously in the Langley 9-inch supersonic tunnel are presented in figure 1(a) to show how the

shocks on a triangular wing may appear. At an angle of attack  $\alpha$  of  $4^\circ$ , the shocks are seen to be considerably different from those at an angle of attack of  $0^\circ$ . The explanation for the presence and structure of such shocks is generally conceded to lie in the similarity of the flow over triangular wings having subsonic leading edges (or supersonic leading edges if the bow wave is unattached) to the flow over two-dimensional airfoils at transonic speeds. From this similarity and the existing knowledge of experimental loading over triangular wings, the shocks shown in figure 1(a) might be expected to appear as shown in figure 1(b) when viewed in the indicated section. The available results of flow studies, as well as investigations of loading, show that the formation of shock waves on triangular wings is varied and complex and may not be associated simply with any single parameter of the flow or of the wing. Further, the surface pressures are known to be considerably altered from the theoretical pressures by these shocks, so that reliable predictions of the loading are prevented. Confirmation of the suspected structure and location of these shocks should aid in attempts to eliminate their detrimental effects. The purpose of this report is to present a technique whereby these shocks and other phenomena in conical fields may be observed in a plane normal or nearly normal to the axis of propagation, and to show some results obtained in an application of the technique to a triangular wing.

#### DESCRIPTION OF METHOD AND TESTS

Basically, the technique is a form of shadowgraphy in which a conical light field is projected against a screen within the test section of the tunnel. The light field must be conical since the flow field about the configurations to which the system is to be applied is conical: that is, the flow has the same physical properties along every straight line passing through the real or fictitious apex of the configurations. (For a cone or thin triangular wing, the apex is real.) For configurations with conical flow fields, the assumption is made that any phenomena which occur in the field will also be conical and that their apexes, if not coincident with the real apex of the configuration, can be approximated satisfactorily.

A conical light field whose apex is adjustable in space within the test section of the tunnel may be easily obtained by a number of methods; two such methods that have been used successfully in tests are described briefly herein. The desired properties for a satisfactory screen presented the problem of obtaining a screen that would cover most of the cross-sectional area of the test section but would cause no choking or intermittent choking of the tunnel flow. One solution to this problem seemed to be a flat-faced propeller rotating in a plane normal to the free-stream direction and allowing passage of the supersonic flow. In

preliminary tests the propeller was driven by its own aerodynamic loading through the use of very slight bevels on one edge. Although these tests were usually satisfactory, certain objectionable qualities such as over-speeding, lack of speed control, variation of speed with Mach number, and tendency to reduce speed as a blade crossed a wake made it desirable to convert the propeller to a motor-driven unit having variable speed control. The variable speed control was particularly advantageous in that it permitted selection of the speed which gave best definition of the image on the propeller screen. The propeller was made of magnesium to reduce inertia loads, and its face was given several coats of matte-white lacquer. The diameter of the propeller was 7.47 inches as compared with the 9-inch-square test section; the cross section of the propeller was rectangular, 0.25 inch by 0.34 inch.

Tests were first made with a cone having a semiapex angle  $\epsilon$  of  $15^\circ$  primarily to prove the technique, since the conical shock from the cone represented a simple predictable phenomenon that should be indicated readily by use of a shadowgraph in the form of a circle on the propeller screen. The cone was mounted on a strut attached to a plate replacing one of the test-section windows (see fig. 2) so that the axis of the cone coincided with the center line of the tunnel. The distance between the tip of the cone and the propeller screen was approximately 4.11 inches. For these tests a General Electric miniature No. 166 "Pilling Grain-of-Wheat" lamp was utilized as the point-source of the conical light field. In a portion of these tests the lamp was mounted within the cone, barely protruding from the apex of the cone as shown in figure 2(a). Essentially, therefore, the cone had a slight rounding of its nose. Other tests were made with a slender mount holding the lamp ahead of the apex of the cone, as shown in figure 2(b).

The main tests were made with a half-span model of an 8-percent-thick triangular wing having a semiapex angle  $\epsilon$  of  $38^\circ$  and an 18-percent-chord location of maximum thickness. The root chord for this wing was 3.35 inches. In these tests the setup included an external-light-source system utilizing a mercury-arc lamp and appropriate lenses in conjunction with a mirror located outside the tunnel to obtain the conical light field. (See fig. 3.) The triangular wing could be moved through a range of angle of attack, and an adjustment could be made to the mirror and light source in order to locate properly the focal point of the conical light field at or near the wing apex. Photographs of the phenomena projected on the propeller screen were made with the camera in the position shown in figure 3. (The camera was in the same position for the cone tests.) In order to reduce reflection, the surfaces of the triangular wing were painted a matte black. Tests of the triangular wing were made at Mach numbers  $M$  of 1.62, 1.93, and 2.41 at several angles of attack and Reynolds numbers. In all tests the distance between the trailing edge of the wing ( $\alpha = 0^\circ$ ) and the propeller screen was approximately 2.75 inches.

## RESULTS

## Cone

Shadowgraphs made at a Mach number  $M$  of 2.41 are shown in figure 4. In figure 4(a) a shadowgraph is presented of the results with the grain-of-wheat lamp mounted in the apex of the cone as shown in figure 2(a) and with the propeller not rotating. The cone shock is visible at the outer edge of the propeller. The shadowgraph made with the grain-of-wheat lamp mounted in the slender support ahead of the cone as shown in figure 4(b) was obtained by two exposures: first, an exposure with the grain-of-wheat lamp as the only light to obtain the shadowgraph with the propeller screen in operation, and second, an exposure with the propeller still and the setup illuminated by an external photoflood lamp. The exact cause of the slight distortion in the propeller-screen image is not known but may be due to a worn bearing on the propeller shaft or to distortion through the tunnel window. An advantage of the latter system is that the lamp is shielded except in the downstream direction and a large amount of reflection from the nozzle surfaces and side walls of the tunnel is avoided.

## Triangular Wing

Figure 5 presents a sketch of the half-span wing mounted on the tunnel window. The conical light field can obviously never scan the inboard region of the wing by this method; however, this condition is not important since the phenomenon to be observed rarely, if ever, lies nearer to the wing root than to the leading edge. The degree to which the conical light field covers the outboard portions of the wing, the leading edge, and the field of flow near the leading edge is a relative quantity subject to several variations at the choice of the operator. These variations include changes in the focal length, focal point, and direction of the conical light field by relative variations of the positions of the light source, mirror, or light-source lenses. This flexibility permits the system to be adjusted to changes in angle of attack of the model, spread or shift of the phenomena, and changes in location of the apparent focal point of the phenomena. The approximate maximum coverage of the wing by the light field for the present tests is indicated in figure 5(a) in terms of the ratio of the fraction of the span covered by the light field to the semispan  $\frac{y}{b/2}$ .

Consider now the actual wing employed to demonstrate the technique (8 percent thick, 18-percent-chord location of maximum thickness). Since the wing does not approach zero thickness, observations can be made of

the phenomena on one surface only. Only for wings having a maximum thickness of the order of the diameter of the focal point of the conical light field is observation of both surfaces possible. The present tests were made in a manner to permit observation of the phenomena on the low-pressure surface of the wing; consequently, the axis of the conical light field was always at a greater negative angle of attack than the wing and the axis of the light field always lay approximately in an extension of the plane of the wing surface behind the ridge line as illustrated in figure 5(b).

Because the flow about such a wing is not truly conical, it was necessary to determine the proper location of the apex of the conical light field by trial-and-error adjustment within a small region of the plane of the wing surface behind the ridge line close to the apex of the wing. In the course of such adjustments, the image on the propeller screen showed no tendency to alter its pattern or structure, the change being one of definition. The location giving best definition of the phenomena was assumed to be the one desired since it corresponds to the greatest length of density gradient traversed by the light rays.

With the aforementioned limits applied to the location of the focal point of the conical light field, the shadow that the wing casts upon the propeller screen may be readily visualized. Since all observations were made at negative angles of attack and the observations were restricted to the low-pressure surface, the lower surface of the wing will appear as the horizontal border of the wing shadow, whereas the leading edge of the wing (which is of no consequence in the observations) will appear, if visible, as the upper border of the wing shadow forming an acute or obtuse angle at the wing tip, depending upon whether it was necessary to locate the focal point of the conical field slightly outboard or slightly inboard, respectively, of the wing leading edge.

Figure 6 presents some examples of the results obtained. The Reynolds number  $R$  and angle of attack  $\alpha$  are given beneath each photograph. (The white circle shown in some of the photographs is the hub of the propeller screen.) Although these tests were made primarily to prove the technique, some interesting observations may be made from the photographs.

At a Mach number of 1.62 and a ratio of tangent of semiapex angle to tangent of Mach angle of 0.995 (fig. 6(a)), the phenomenon is seen to progress from a shock almost normal to the wing surface at  $\alpha = -8^\circ$  to a pattern of lambda shocks at more negative angles of attack. Available results of flow studies on triangular wings seem to indicate that, as the angle of attack is increased, the shocks on the high-pressure surface of the wing would disappear and that those on the low-pressure surface would take the form of lambda shocks. The latter condition appears to

be confirmed by the results at  $\alpha = -10^\circ$ , in particular; it is interesting to note the similarity of this shock pattern to a concept by C. E. Brown of the Langley Laboratory of the flow over the triangular wing shown in figure 7. The apparent crossing of the shocks seen in figure 6, which tends to occur at the more negative angles of attack, seems to contradict the possible shock patterns. The observed shock patterns could be brought about by a peculiar path of a single shock along the wing surface.

At a Mach number of 1.93 and a ratio of tangent of semiapex angle to tangent of Mach angle of 1.29 (fig. 6(b)), a view at  $\alpha = 0^\circ$  is presented to show the appearance and proximity of the bow wave which is detached because of the large wedge angle at the wing leading edge. This particular photograph was taken with the focal point of the light field coincident with the apex of the wing. The photographs at angle of attack show again the complex patterns of the phenomena.

At a Mach number of 2.41 and a ratio of tangent of semiapex angle to tangent of Mach angle of 1.71 (fig. 6(c)), the bow wave is seen to be very close to attachment at  $\alpha = 0^\circ$ . At the lower angles of attack, the surface shocks and bow wave may be viewed simultaneously; here the surface shocks do appear to form a lambda shock. Although not recorded, observations indicated this condition to hold at the larger angles of attack. A distinct increase in the inclination of the surface shocks with angle of attack is shown; this result is also noticeable at the other Mach numbers, but the effect appears to decrease with decreasing Mach number.

At all Mach numbers, the results are indicated to be associated with separation at the wing leading edge or ridge line. This separation is visible in a number of the photographs. Also indicated is the inboard movement of the base of the shocks with increasing angle of attack.

On the basis of these limited tests, it would seem reasonable to conclude that the propeller-screen technique is satisfactory for observing the shock and separation phenomena that may exist on triangular wings. In addition, the results appear to support the general conceptions of the similarity between the flow over two-dimensional airfoils at transonic speeds and the flow at supersonic speeds over triangular wings with subsonic leading edges.

#### POSSIBLE VARIATIONS OF THE METHOD

Applications other than the two previously described can obviously be made. One application in particular which appears to have promise

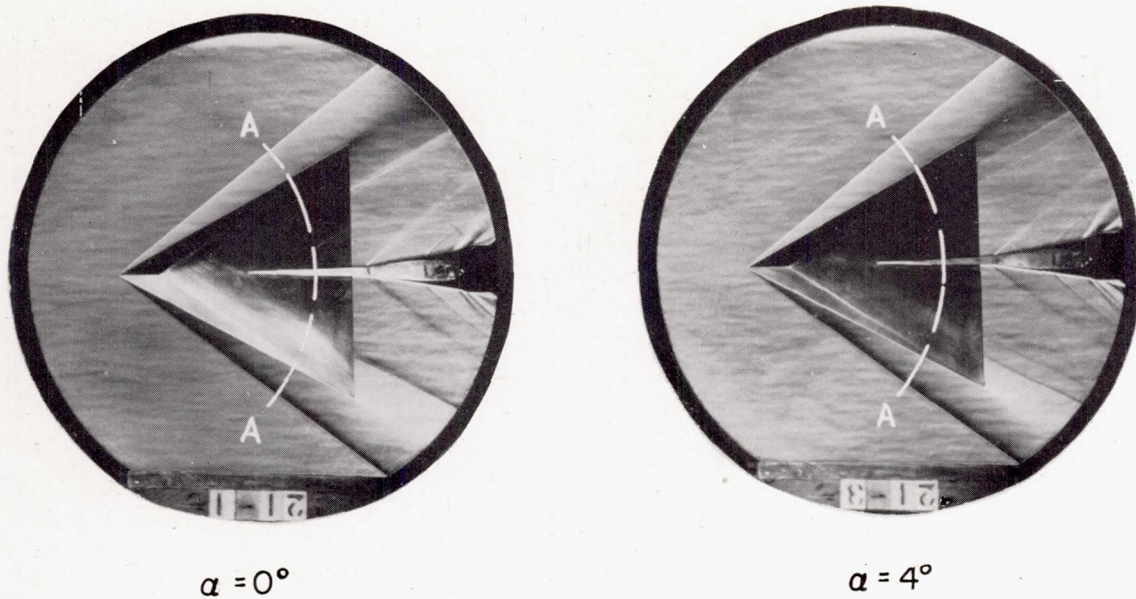


is the use of full-span triangular wings and of light fields that cover the entire wing surface. For this arrangement a very slender support (similar to the setup for the cone studies) attached to one surface of the wing would support a very small mirror, or prism, whose size is of the order of the focal point of the conical light field. This mirror would lie at the focal point of the phenomena and the light field and would turn the light through  $90^\circ$ , so that the light would enter the test section at  $90^\circ$  to stream direction. Consequently, very wide conical light fields could be realized. To avoid distortion caused by photographing the image through the tunnel window, tunnels of sufficient size might use a camera mounted downstream of a translucent Plexiglass propeller screen to photograph the reverse of the image. This technique has been successfully demonstrated in bench tests. The propeller screen may be made more uniform with respect to lighting by masking the face of the propeller with matte black such that the matte-white area is tapered toward the center of rotation.

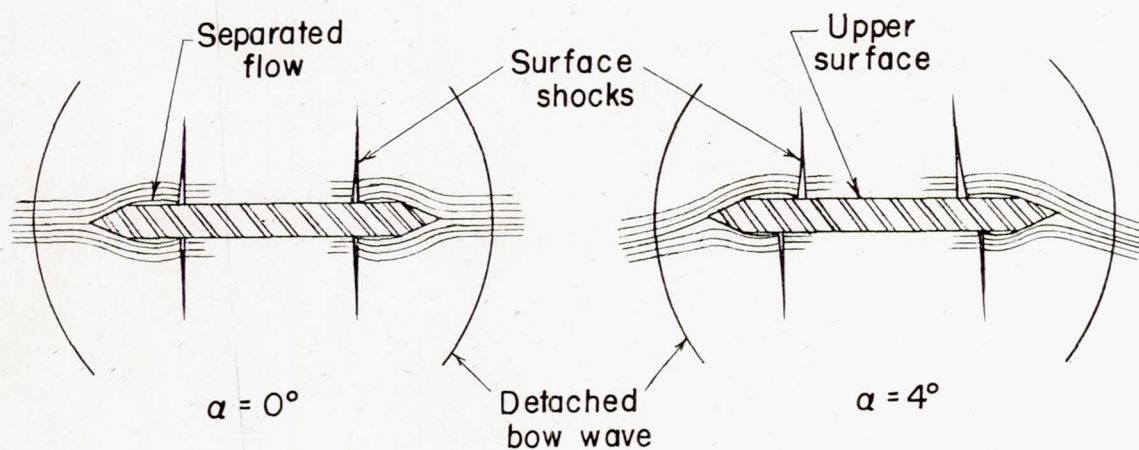
#### CONCLUDING REMARKS

A new shadowgraph technique for the observation of conical flow phenomena in supersonic flow has been presented. The particular advantage of this technique over conventional types of shadowgraph or schlieren systems is that it permits observation of the phenomena in a plane normal or nearly normal to the axis of propagation. Preliminary tests with a triangular wing gave satisfactory results.

Langley Aeronautical Laboratory,  
National Advisory Committee for Aeronautics,  
Langley Field, Va., February 24, 1953.



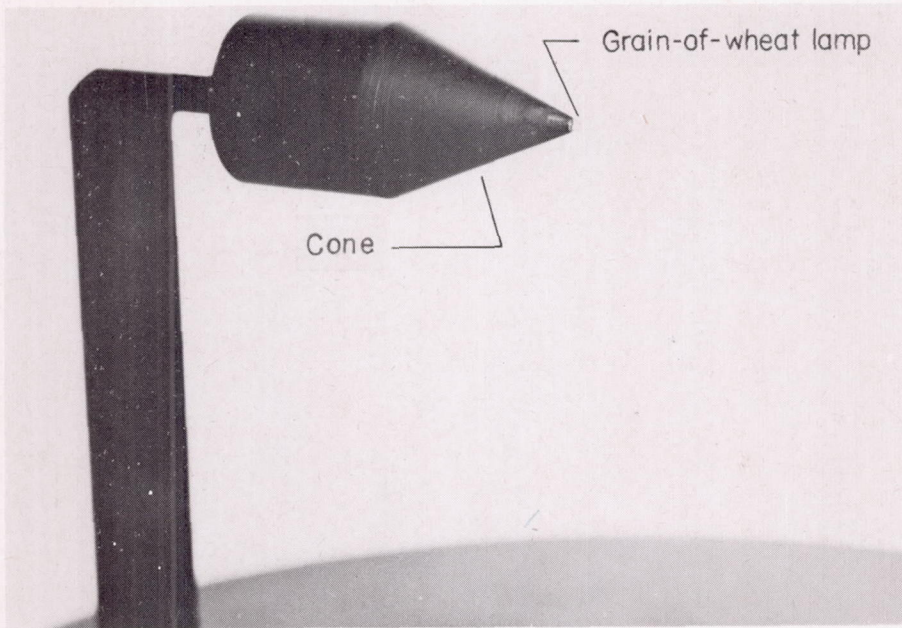
(a) Schlieren photographs.



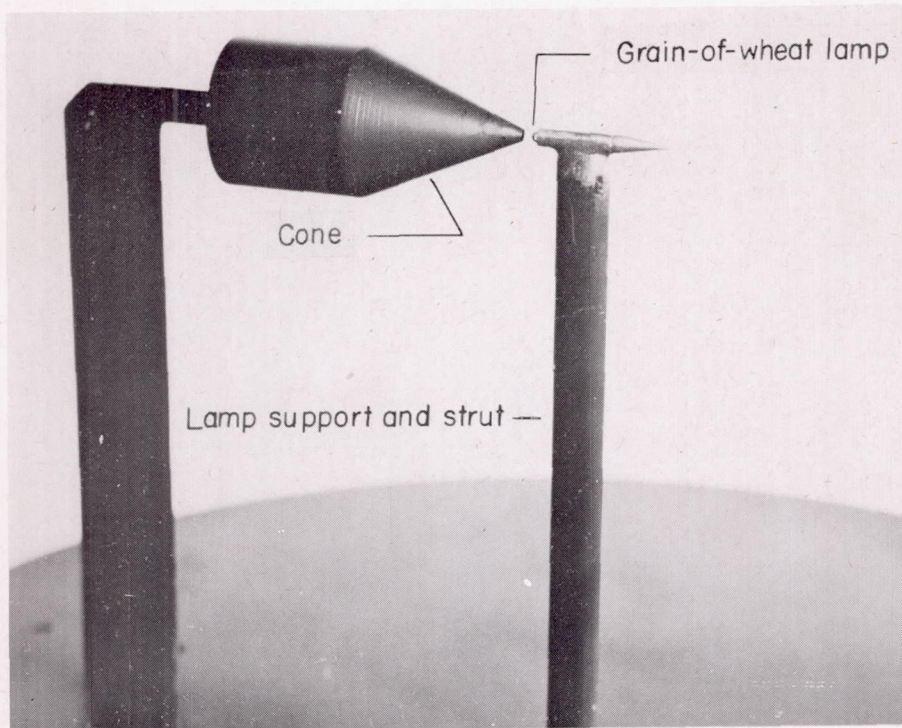
(b) Conception of flow phenomena at radial section A-A.

NACA  
L-79186

Figure 1.- Examples of surface shocks occurring on a triangular wing at  $M = 1.93$ . Wing is 8 percent thick with 18-percent-chord location of maximum thickness. Ratio of tangent of semiapex angle to tangent of Mach angle  $\tan \epsilon / \tan \mu$ , 0.864.

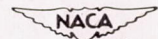


(a) Grain-of-wheat lamp mounted in apex of cone.



(b) Grain-of-wheat lamp mounted in slender strut ahead of cone.

Figure 2.- Photographs of cone and grain-of-wheat lamp. L-79187



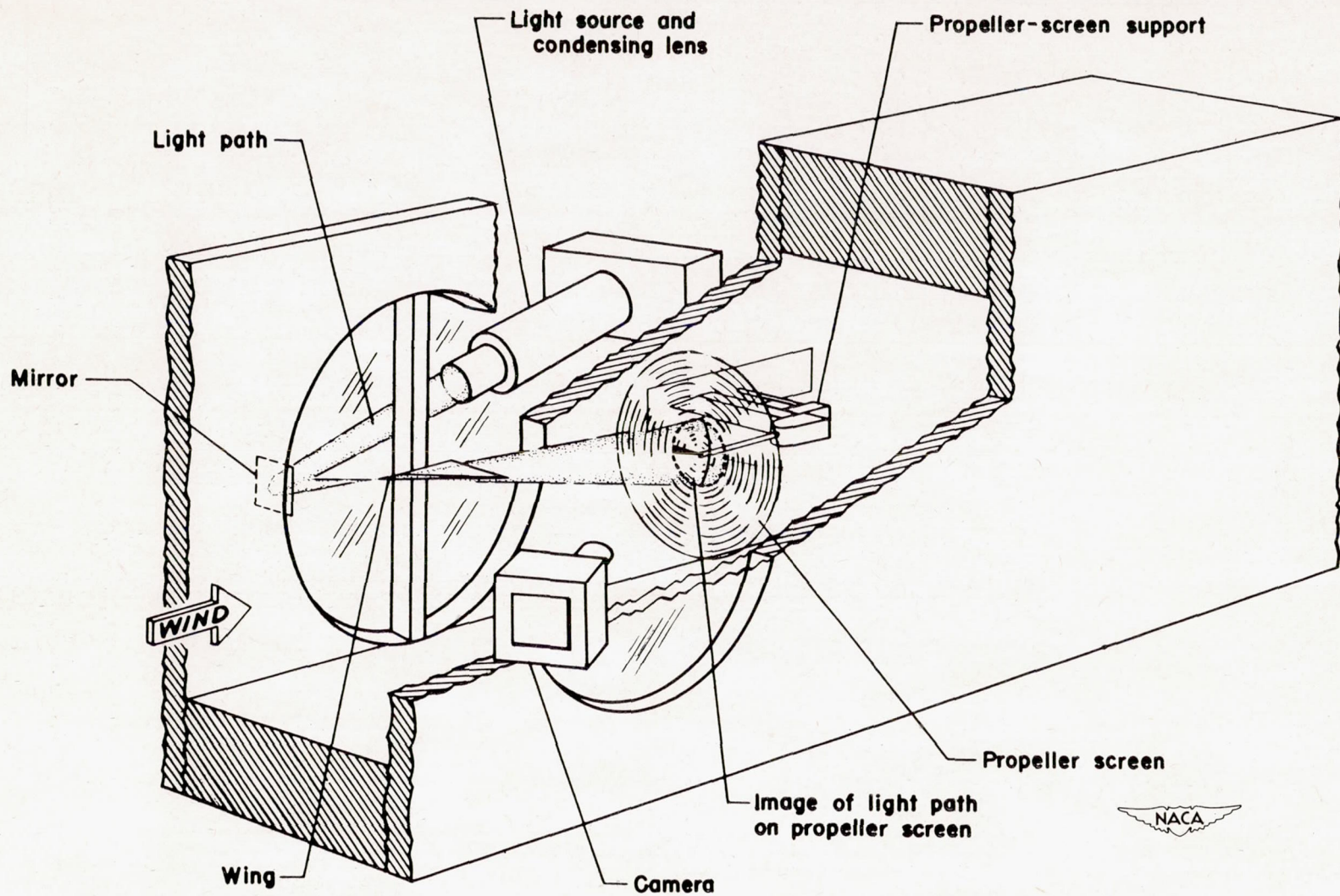
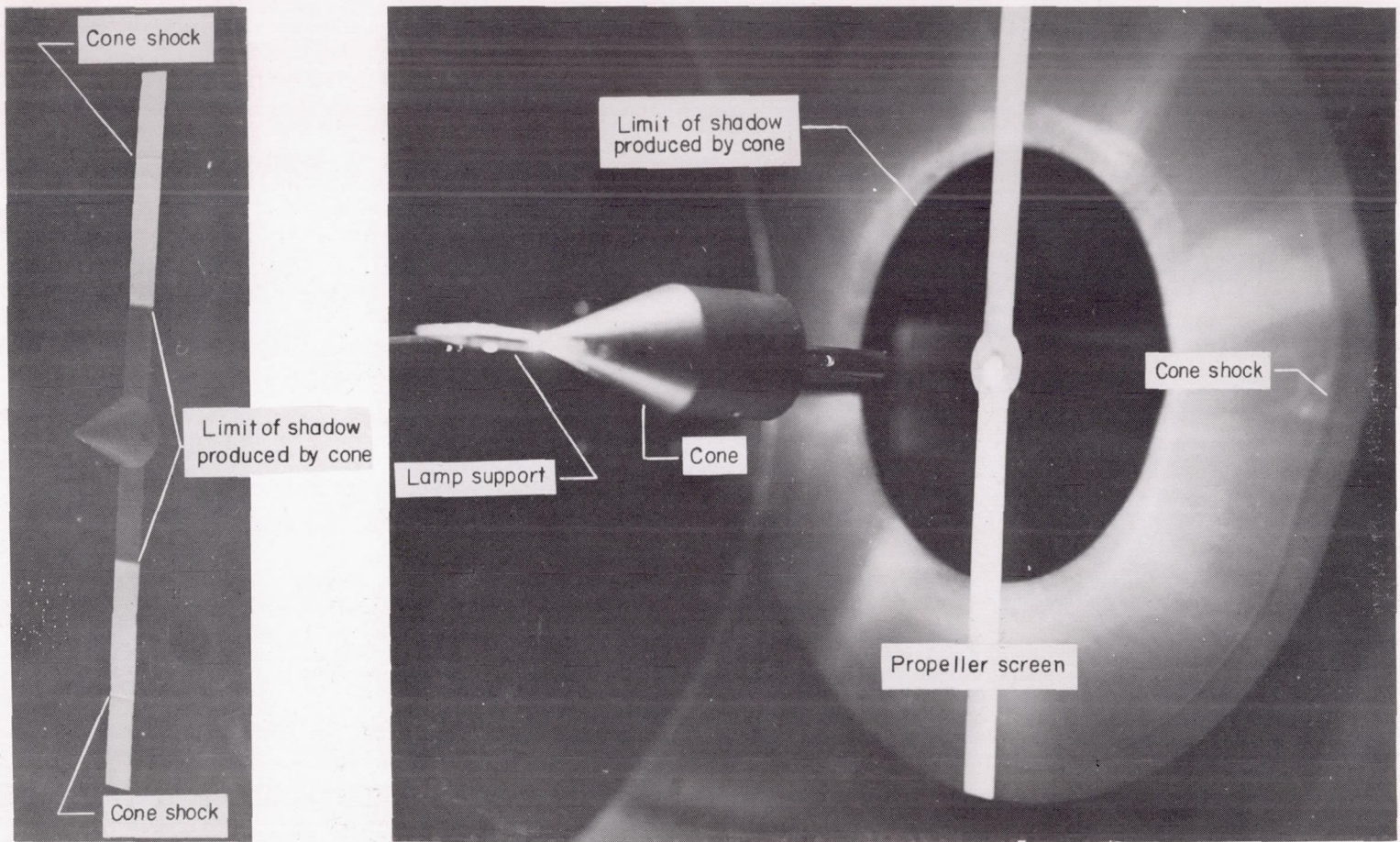


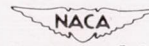
Figure 3.- Drawing of conical shadowgraph system utilizing a half-span triangular wing and external light source.



(a) Grain-of-wheat lamp in apex of cone.

(b) Grain-of-wheat lamp in support ahead of cone.

Figure 4.- Shadowgraphs of cone shock.  $M = 2.41$ . L-79188



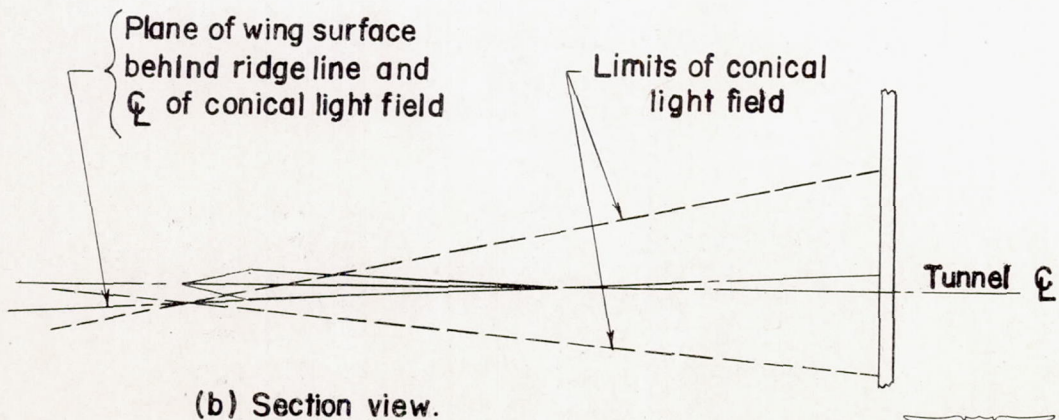
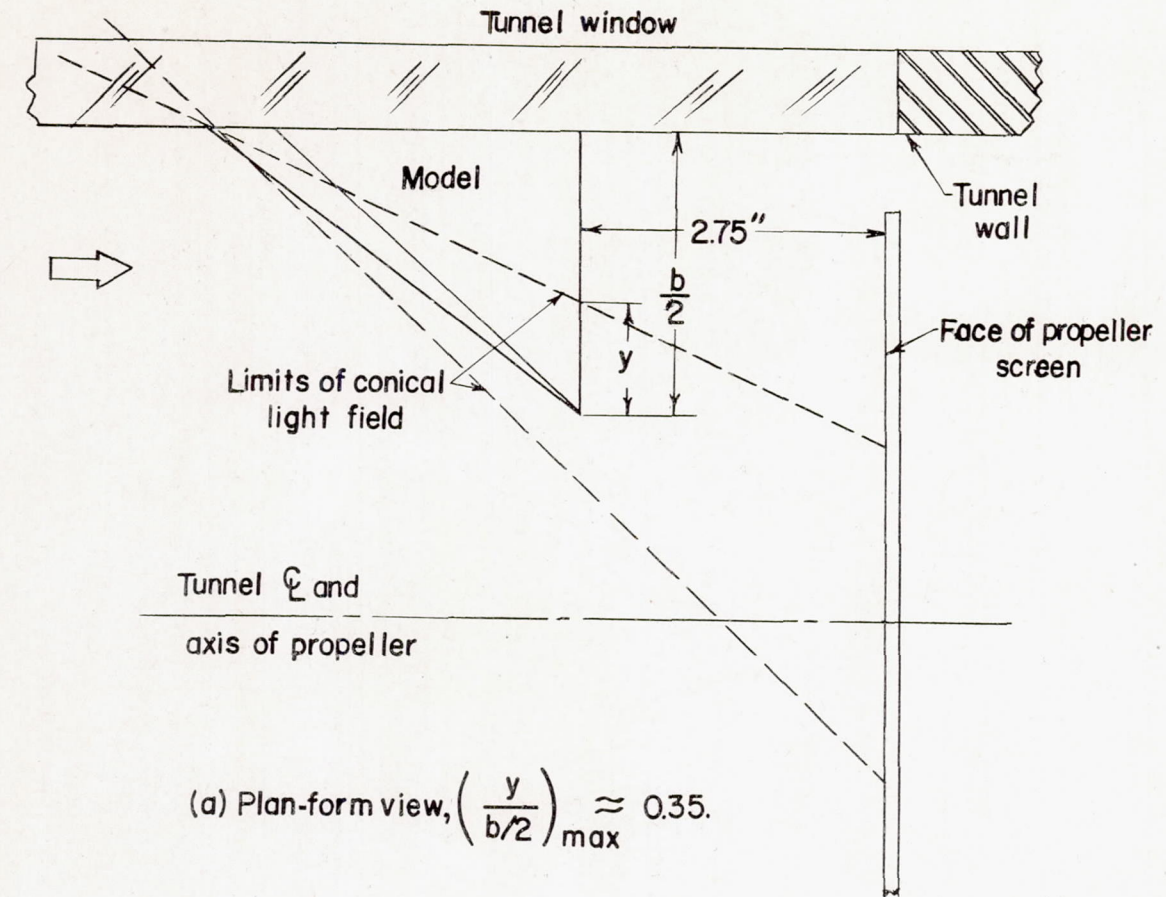
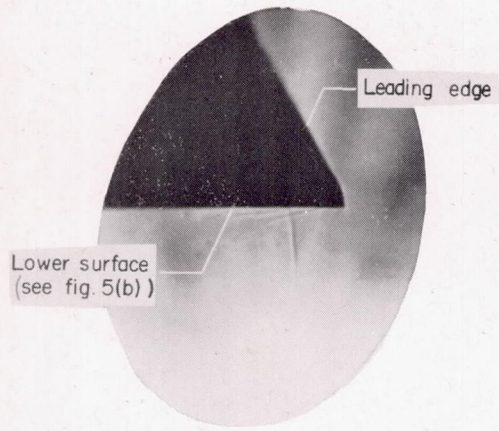
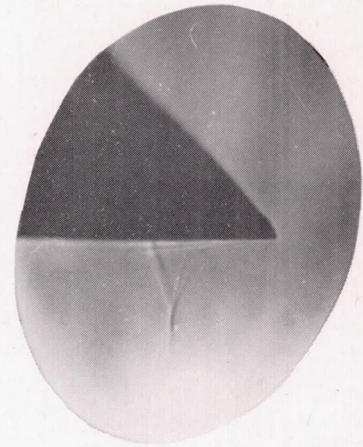


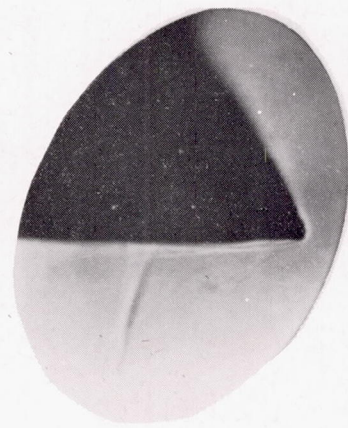
Figure 5.- Sketch of relation between light field, wing model, and propeller screen.



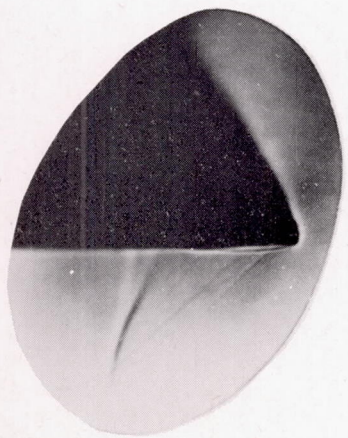
$\alpha = -8^\circ$   
 $R = 0.37 \times 10^6$  per in.



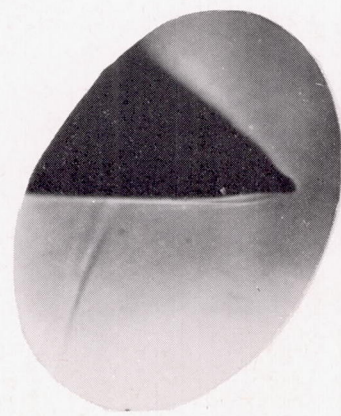
$\alpha = -10^\circ$   
 $R = 0.37 \times 10^6$  per in.



$\alpha = -12^\circ$   
 $R = 0.37 \times 10^6$  per in.

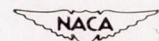


$\alpha = -12^\circ$   
 $R = 0.70 \times 10^6$  per in.



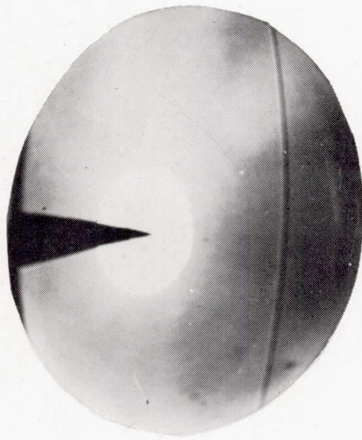
$\alpha = -14^\circ$   
 $R = 0.37 \times 10^6$  per in.

(a)  $M = 1.62.$

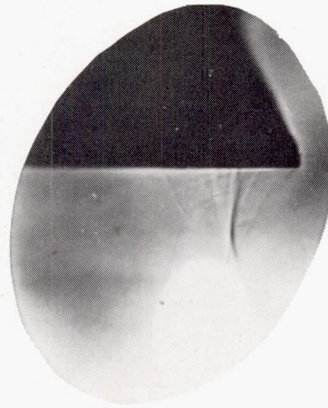


L-79189

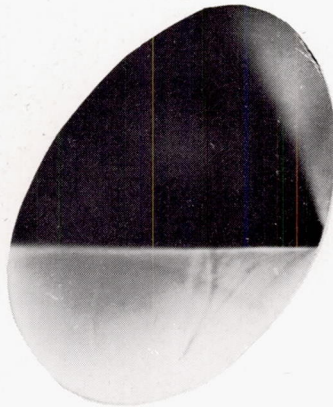
Figure 6.- Shadowgraphs of flow phenomena on low-pressure surface of triangular wing of  $38^\circ$  half-apex angle.



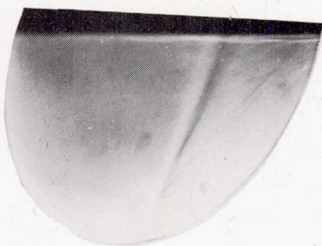
$\alpha = 0^\circ$   
 $R = 0.63 \times 10^6$  per in.



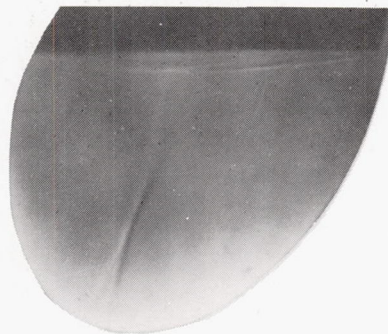
$\alpha = -6^\circ$   
 $R = 0.63 \times 10^6$  per in.



$\alpha = -8^\circ$   
 $R = 0.63 \times 10^6$  per in.



$\alpha = -10^\circ$   
 $R = 0.63 \times 10^6$  per in.



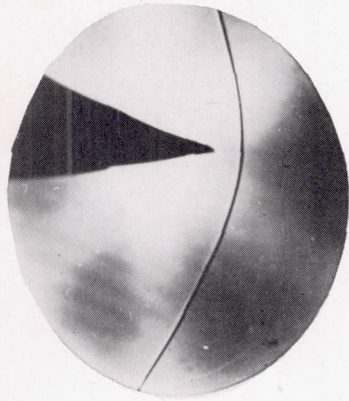
$\alpha = -12^\circ$   
 $R = 0.63 \times 10^6$  per in.

(b)  $M = 1.93$ .

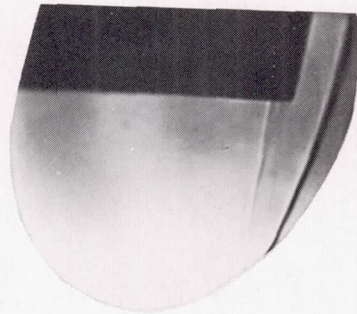


Figure 6.- Continued. L-79190

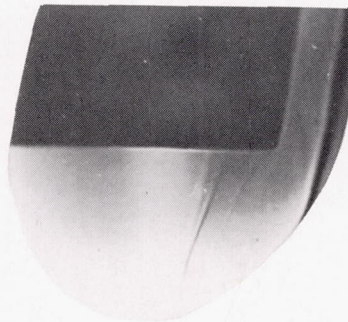




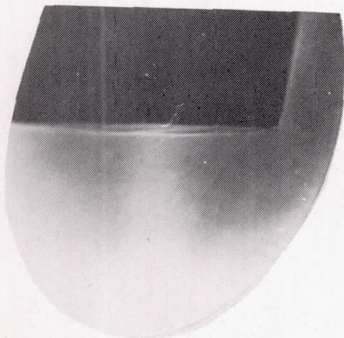
$\alpha = 0^\circ$   
 $R = 0.26 \times 10^6$  per in.



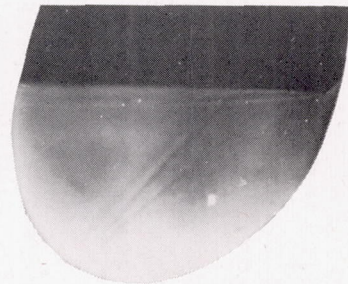
$\alpha = -4^\circ$   
 $R = 0.73 \times 10^6$  per in.



$\alpha = -6^\circ$   
 $R = 0.73 \times 10^6$  per in.



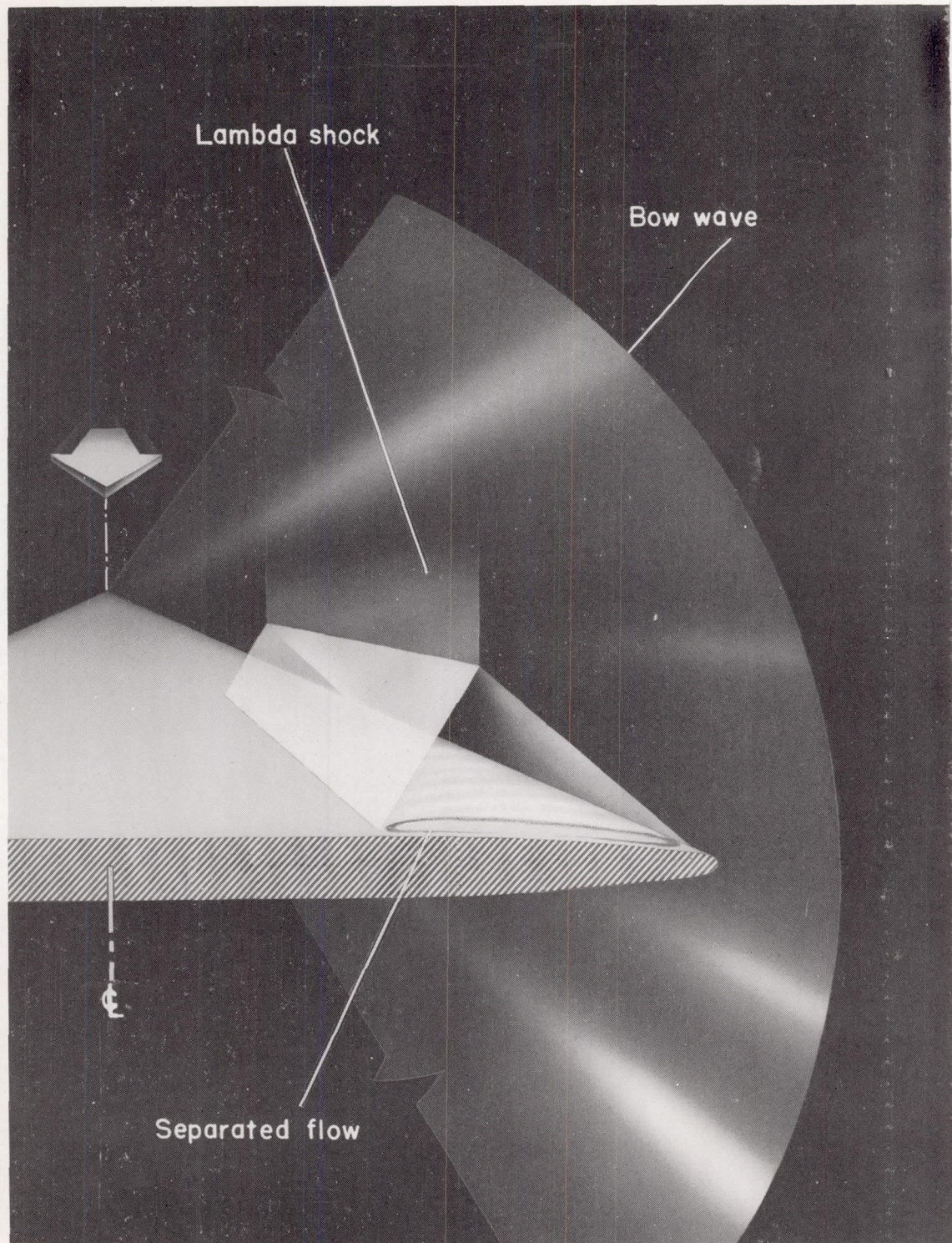
$\alpha = -10^\circ$   
 $R = 0.73 \times 10^6$  per in.



$\alpha = -14^\circ$   
 $R = 0.73 \times 10^6$  per in.

(c)  $M = 2.41$ .

Figure 6.- Concluded.



NACA

L-79192

Figure 7.- Conception of flow over upper surface of triangular wing.  
Wing has rounded leading edges and streamwise airfoil sections based  
on NACA 00-series airfoils.  $\alpha = 10^\circ$ ;  $M = 2.41$ ;  $\tan \epsilon / \tan \mu = 0.867$ .